Arthritis Research & Therapy

RESEARCH

Open Access

Brain functional alternation in patients with systemic sclerosis: a resting-state functional magnetic resonance imaging study

Xinyu Tong[1†], Huilin He[2†], Shihan Xu[2], Rui Shen[3], Zihan Ning[3,4], Xiaofeng Zeng[2], Qian Wang[2], Dong Xu[2*], Zuo-Xiang He[1*] and Xihai Zhao[3*]

Abstract

Background Neuropsychiatric manifestations, such as cognitive impairment, are relatively prevalent in systemic sclerosis (SSc) patients. This study aimed to investigate the resting state (RS) functional alternations of SSc patients and the potential influenced factors.

Methods Forty-four SSc patients (mean age, 46.3 ± 11.4 years; 40 females) and 19 age and sex comparable healthy volunteers (mean age, 42.6 ± 11.3 years; 16 females) were recruited and underwent RS functional MR imaging (fMRI) and neuropsychological assessments. Functional segregation analysis was performed to calculate the amplitude of low frequency fluctuation (ALFF) and regional homogeneity (ReHo). Functional integration analysis was conducted using group independent component analysis to calculate intra-network and inter-network functional connectivity (FC). The fMRI measurements were compared between SSc patients and healthy volunteers using voxel-based pairwise two-sample *t*-tests. The correlations between clinical characteristics and fMRI measurements were also analyzed.

Results Compared to healthy volunteers, SSc patients exhibited significantly decreased ALFF and increased ReHo (all $P < 0.01$, FWE corrected). SSc patients predominantly showed decreased intra-network and inter-network FC in the auditory network, visual network, default mode network, frontoparietal network and attention network (intra-network FC: $P < 0.01$, uncorrected, cluster size > 30; inter-network FC: $P < 0.05$, FDR correction). Furthermore, clinical characteristics including disease duration (r value ranged from −0.31 to 0.36), elevated erythrocyte sedimentation

†Xinyu Tong and Huilin He are co-first authors and contributed equally to this study.

†Zuo-Xiang He, Dong Xu and Xihai Zhao are co-corresponding authors and equally contributed to this study.

*Correspondence:
Dong Xu
xudong74@hotmail.com
Zuo-Xiang He
zuoxianghe@hotmail.com
Xihai Zhao
xihaizhao@tsinghua.edu.cn

Full list of author information is available at the end of the article

© The Author(s) 2024. **Open Access** This article is licensed under a Creative Commons Attribution-NonCommercial-NoDerivatives 4.0 International License, which permits any non-commercial use, sharing, distribution and reproduction in any medium or format, as long as you give appropriate credit to the original author(s) and the source, provide a link to the Creative Commons licence, and indicate if you modified the licensed material. You do not have permission under this licence to share adapted material derived from this article or parts of it. The images or other third party material in this article are included in the article's Creative Commons licence, unless indicated otherwise in a credit line to the material. If material is not included in the article's Creative Commons licence and your intended use is not permitted by statutory regulation or exceeds the permitted use, you will need to obtain permission directly from the copyright holder. To view a copy of this licence, visit http://creativecommons.org/licenses/by-nc-nd/4.0/.

rate ($r = 0.35$), Montreal Cognitive Assessment score ($r = 0.43$), and Hamilton Depression Scale score ($r = -0.40$) were significantly associated with fMRI measurements (all $P < 0.05$).

Conclusions Spontaneous activity and functional connectivity alternations can be seen in SSc patients, which are partially associated with neuropsychiatric manifestations and tend to aggravate with disease duration.

Keywords Systemic sclerosis, Brain, Resting state fMRI, Independent component analysis

Background

Systemic sclerosis (SSc) is one of the systemic autoimmune diseases characterized by immune dysregulation, vasculopathy and progressive fibrosis [1]. SSc frequently involves multiple organs, including the skin, lung, heart, gastrointestinal tract and kidneys [2–4]. Although brain involvement was once considered as atypical patterns in SSc, recent studies have increasingly focused on brain involvement in these patients [5–7]. Besides encephalopathy, seizures and vasculitis, the presence of neuropsychiatric manifestations such as depression, anxiety and cognitive impairment has also been reported in SSc patients [8–10]. Notably, up to 61% of SSc patients were found to have mild cognitive impairment [11]. However, the specific patterns of brain functional alternations which might be linked to these neuropsychiatric manifestations still remain poorly understood.

Resting state (RS) functional MR imaging (fMRI) is a promising imaging tool for investigating the neural mechanisms of neuropsychiatric disorders that are not visible on structural imaging. The analytic approaches of RS fMRI included functional segregation and functional integration methods [12]. The functional segregation method focuses on the local function of specific brain regions, while the functional integration method focuses on the functional connectivity (FC). Previous studies have reported the presence of local function and connectivity abnormalities in other systemic rheumatic diseases, such as systemic lupus erythematosus (SLE) and rheumatoid arthritis (RA), and revealed an association between these functional abnormalities and both inflammation and neuropsychiatric manifestations [13–15]. Therefore, we hypothesized that similar pathophysiological mechanism and functional abnormalities may also exist in SSc patients, potentially contributing to their neuropsychiatric manifestations.

This study aimed to investigate the RS functional alternations in SSc patients using both segregation and integration methods from fMRI images. Furthermore, this study also sought to determine the association of these functional alternations with clinical characteristics, to explore the underlying influenced factors of brain involvement in SSc patients.

Methods

Study population

In this cross-sectional observational study, SSc patients and healthy volunteers with comparable age and sex were recruited. The inclusion criteria for the SSc patients were as follows: (1) meeting the 2013 American College of Rheumatology/European League Against Rheumatism criteria [16]; (2) age ranged 18–70 years old; (3) having more than 6 years of education; (4) being right-handed; (5) having normal or corrected-to-normal vision. The exclusion criteria for SSc patients were: (1) coexisting with other autoimmune disease, such as SLE and RA; (2) having a history of confirmed central nervous diseases, such as stroke, epilepsy, cerebral parenchymal lesions, cerebrovascular diseases, severe active mental illness, or traumatic brain injury; (3) taking concomitant medications that could cause an organic mental syndrome; (4) having a history of established psychiatric/mental disorders; and (5) having contraindications to MR examination. All patients and healthy volunteers underwent brain MR imaging within one week after recruitment. The study protocol was approved by institutional review board and written consent form was obtained from all patients and healthy volunteers before participation.

Clinical information collection

Demographic information, including age, sex, and body mass index (BMI), was collected from both SSc patients and healthy volunteers. Disease-related clinical characteristics including SSc subsets (limited cutaneous (lc) and diffuse cutaneous (dc)), disease duration, clinical manifestations, modified Rodnan skin score (mRSS) and blood biomarkers were also collected. The clinical manifestations included: (1) Raynaud's phenomenon; (2) digital ulcers (DU); (3) digital gangrene; (4) interstitial lung disease (ILD); (5) pulmonary arterial hypertension; (6) gastroesophageal reflux; and (7) scleroderma renal crisis. The collected blood biomarkers were as follows: (1) inflammatory biomarkers: erythrocyte sedimentation rate (ESR) (values > 20 mm/h were considered abnormally elevated) and high-sensitivity C-reactive protein; (2) immunoglobulins: immunoglobulin G, immunoglobulin A, and immunoglobulin M; and (3) autoantibodies: antinuclear antibody (ANA), anticentromere antibody, anti-double-stranded DNA antibody, anti-ribonucleoprotein antibody, anti-Sjögren Syndrome A/B antibodies,

and anti-topoisomerase antibody. Additionally, all SSc patients underwent the Hamilton Anxiety Scale (HAMA) [17], Hamilton Depression Scale (HAMD) [18], and Montreal Cognitive Assessment (MoCA) [19] tests to assess the levels of anxiety, depression, and cognitive function, respectively.

Brain MR imaging

Brain 3D T1-weighted (T1w) MR imaging and RS fMRI were performed for all the patients and healthy subjects on a 3T MR scanner (Ingenia CX, Philips Healthcare, Best, The Netherlands) with a 64-channel head coil. The 3D T1w images were acquired using a magnetization prepared rapid gradient echo sequence with the following parameters: repetition time=8.2 ms, echo time=3.8 ms, flip angle=8°, field of view=256×256×160 mm^3, voxel size=1×1×1 mm^3, number of slices=160, axial orientation, compressed sensing-sensitivity encoding acceleration factor=3, and scan time=2 min 03 s. The RS fMRI images were acquired using a T2*-weighted echo-planar imaging sequence with the following parameters: repetition time=2000 ms, echo time=30 ms, flip angle=90°, field of view=256×256×136 mm^3, voxel size=3.5×3.5×3.5 mm^3, number of slices=34, axial orientation, and scan time=8 min 6 s. All subjects were instructed to remain motionless, without thinking anything or falling asleep during fMRI scanning.

Image pre-processing

The pre-processing of fMRI data was performed using the RS fMRI Data Analysis Toolkit plus V1.28 (REST-plus V1.28) in the Matlab R2022a (The Mathworks, Natick, MA) environment. The data pre-processing steps included: (1) removing the first five volumes of each time series; (2) slice timing correction with the 18th slice as the reference; (3) realignment of head motion using a rigid spatial transformation; and (4) spatial normalization using a two-step registration, where the fMRI images were registered to each subject's T1w images and then registered to the Montreal Neurological Institute (MNI) space and resampled to a voxel size of 3×3×3 mm^3. Additionally, subjects with excessive head motion in any direction (>3 mm or 3°) were excluded from the analysis.

To calculate the amplitude of low frequency fluctuation (ALFF), three additional three steps were applied to the normalized fMRI images: (1) spatial smoothing with a 6-mm full-width half-maximum (FWHM) Gaussian kernel; (2) linear detrending; and (3) removing nuisance components, including 24-parameter head motion, the white matter signal, and the cerebrospinal fluid signal using temporal linear regression.

To calculate the regional homogeneity (ReHo), the following three additional three steps were performed: (1) linear detrending; (2) temporal linear regression as described in the ALFF pre-processing; and (3) temporal filtering with a frequency range of 0.01–0.08 Hz.

ALFF and ReHo calculation

For ALFF calculation, the temporal series were transformed into the frequency domain using a fast Fourier transform. The square root of the power spectrum was then calculated at each frequency, and the average square root across the 0.01–0.08 Hz was taken as the ALFF for each voxel. For fALFF calculation, the power within the low-frequency range (0.01–0.08 Hz) was divided by the power of the entire frequency range. Both ALFF and fALFF were then normalized by dividing each voxel's value by the respective global mean, resulting in mean ALFF (mALFF) and mean fALFF (mfALFF) spatial maps for further statistical analysis.

For ReHo calculation, the Kendall's correlation coefficient (Kcc) was computed for each voxel and its 26 neighboring voxels. Each Kcc map was then standardized by dividing its global mean Kcc value. The standardized Kcc maps were subsequently smoothed with a 6-mm FWHM Gaussian kernel to produce smKccReHo maps for further statistical analysis.

Group independent component analysis

Group independent component analysis (ICA) was performed on preprocessed fMRI data using the GIFT 4.0b toolbox (http://mialab.mrn.org/software/gift). The nu mber of independent components (ICs) was estimated as 46 using the minimum description length criteria. To assess the reliability of these ICA estimates, the software ICASSO (http://research.ics.tkk.fi/ica/icasso/) was employed, which utilized 100 repetitions of the Infomax algorithm to construct aggregated spatial map. These aggregate maps were compared to established RS networks [20] through spatial correlation values and visual inspection, discarding those corresponding to physiological noise and motion artifacts. Ultimately, 20 ICs were selected and classified into 13 RS functional networks: auditory network (AN); medial, lateral, and posterior visual networks (mVN, lVN, and pVN); dorsal and ventral sensorimotor networks (dSMN and vSMN); salience network (SN); anterior and posterior default mode networks (aDMN and pDMN); left and right frontoparietal networks (lFPN and rFPN); dorsal and ventral attention networks (DAN and VAN), as shown in Fig. 1.

Intra-network FC within these networks was subsequently analyzed. To explore relationships between ICs, functional network connectivity (FNC) analysis was conducted using the GIFT 4.0b toolbox. The time courses of each subject underwent initial detrending and despiking based on the median absolute deviation, followed by high pass filtering with a cutoff frequency of 0.15 Hz. Pearson's correlation coefficients between pairs of time courses

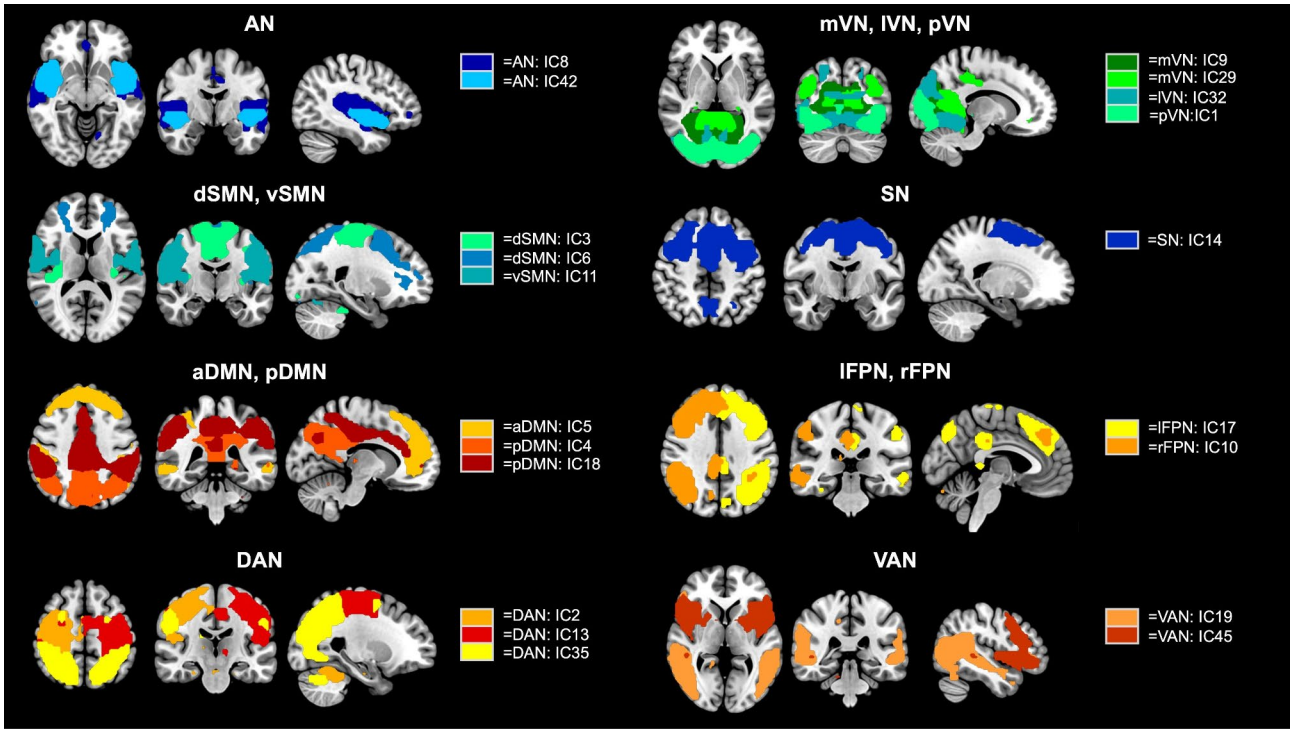

Fig. 1 Spatial maps of the 20 independent components (ICs). 20 ICs were selected and classified into 13 resting state networks: auditory network (AN: 2 ICs); medial, lateral, and posterior visual networks (mVN: 2 ICs, lVN: 1 IC, and pVN: 1 IC); dorsal and ventral sensorimotor networks (dSMN: 2 ICs and vSMN: 1 IC); salience network (SN: 1 IC); anterior and posterior default mode networks (aDMN: 1 IC and pDMN: 2 ICs); left and right frontoparietal networks (lFPN: 1 IC and rFPN: 1 IC); dorsal and ventral attention networks (DAN: 3 ICs and VAN: 2 ICs)

were computed and transformed into z-scores using Fisher's transformation. A correlation matrix of size n*n (where n represents the number of ICs) was generated for each subject.

Statistical analysis

The continuous variables were presented as mean ± standard deviation (SD) or medians (interquartile range, IQR), while the categorical variables were expressed as counts and frequencies. To compare demographic characteristics between SSc patients and healthy volunteers, independent *t*-tests, Mann-Whitney *U* tests, or Chi-square tests were used. The fMRI measurements were compared using voxel-based statistical analysis with pairwise two-sample *t*-tests, including gender and age as covariates.

In the analysis of ALFF and ReHo, cluster-level statistics were corrected for family-wise error (FWE) at $P<0.01$. For intra-network FC analysis, an uncorrected $P<0.01$ and cluster size > 30 voxels were considered to be significant difference. In the FNC analysis, inter-group comparisons were conducted with false discovery rate (FDR) correction at $P<0.05$. Pearson or Spearman correlation analyses were employed to determine the relationships between clinical characteristics and fMRI measurements extracted from brain regions with significant differences. A Pvalue <0.05 was considered statistically significant.

All statistical analyses were performed using SPSS 27.0 (SPSS Inc. Chicago, IL, USA) and the SPM12 toolbox (https://www.fil.ion.ucl.ac.uk/spm/software/spm12/). The results were visualized using the xjview toolbox (http://www.alivelearn.net/xjview) and MRIcroGL (http://www.mccauslandcenter.sc.edu/mricrogl).

Results

Clinical characteristics

A total of 44 SSc patients and 19 healthy volunteers were recruited. The clinical characteristics are presented in Table 1. Of the 44 SSc patients, the mean age was 46.3 ± 11.4 years old, 40 (90.9%) were females, 23 (52.3%) were diffuse dcSSc patients. The median mRSS for all SSc patients was 4.0 [2.0, 6.8]. Of the 19 healthy volunteers, the mean age was 42.6 ± 11.3 years old, 16 (84.2%) were females. No significant differences were observed in the demographic characteristics (age, sex and BMI) and educational attainment between SSc patients and healthy volunteers (all $P>0.05$). Regarding the medication use, 26 (59.1%) SSc patients had used steroids, while 3 (6.8%) had used vasodilators. Notably, none had received vasoactive treatments or psychiatric medications.

Table 1 Clinical characteristics of study population

	SSc patients (*n* = 44)	Healthy volunteers (*n* = 19)	*P*
Age, years	46.3 ± 11.4	42.6 ± 11.3	0.238
BMI, kg/m^2	22.5 ± 3.6	23.2 ± 2.8	0.467
Gender, female	40 (90.9)	16 (84.2)	0.441
Education, years	14.0 [9.0,16.0]	16.0 [12.0, 16.0]	0.373
disease duration, months	44.5 [16.8, 80.8]	/	/
Subtypes, dcSSc	23 (52.3)	/	/
MoCA score	26.0 [24.0, 28.0]	/	/
HAMA	5.0 [3.0, 7.0]	/	/
HAMD	6.5 [4.0, 10.0]	/	/
mRSS	4.0 [2.0, 6.8]	/	/
PGA	0.7 ± 0.4	/	/
IgG, g/L	13.0 [10.9, 17.4]	/	/
IgA, g/L	2.5 [1.7, 3.7]	/	/
IgM, g/L	1.1 [0.8, 1.6]	/	/
ESR, mm/hour	11.5 [8.0, 30.0]	/	/
Elevated ESR	11 (25.0)	/	/
hsCRP, mg/L	1.15 [0.5, 3.0]	/	/
ANA	42 (95.5)	/	/
ACA	2 (4.5)	/	/
Anti-RNP antibody	8 (18.2)	/	/
Anti-SSA antibody	10 (22.7)	/	/
Anti-SSB antibody	2 (4.5)	/	/
Anti-Scl70 antibody	26 (59.1)	/	/
Raynaud's phenomenon	36 (81.8)	/	/
Digital ulcers	10 (22.7)	/	/
Digital gangrene	2 (4.5)	/	/
Interstitial lung disease	24 (54.5)	/	/
Steroid use	26 (59.1)	/	/
Vasodilatory use	3 (6.8)	/	/

BMI, body mass index; dcSSc, diffuse cutaneous SSc; MoCA: Montreal Cognitive Assessment; HAMA: Hamilton Anxiety Scale; HAMD: Hamilton Depression Scale; mRSS, modified Rodnan skin score; PGA, physician's global assessment; IgG, immunoglobulin G; IgA, immunoglobulin A; IgM, immunoglobulin M; ESR, erythrocyte sedimentation rate; hsCRP, high-sensitivity C-reactive protein; ANA, antinuclear antibody; ACA, anticentromere antibody; Anti RNP, anti-ribonucleoprotein; anti-SSA/SSB, anti-Sjögren Syndrome A/B; Anti Scl-70, anti-topoisomerase

ALFF and ReHo results

Figure 2 shows the comparison results of mALFF, mfALFF and smKccReHo between SSc patients and the healthy volunteers (Table 2). Compared to the healthy volunteers, the SSc patients showed significantly decreased mALFF in putamen part of the right lenticular nucleus, and significantly decreased mfALFF in left inferior temporal gyrus, right middle frontal gyrus and left middle frontal gyrus (all $P<0.01$, FWE corrected). In contrast, SSc patients showed significantly increased smKccReHo in right inferior temporal gyrus and orbital part of right inferior frontal gyrus (all $P<0.01$, FWE corrected).

Intra-network functional connectivity results

Figure 3 illustrates the voxel-wise differences of intra-network FC in the different networks between SSc patients and healthy volunteers (Table 3). Compared to healthy volunteers, SSc patients exhibited significantly decreased FC in the right insula and right Rolandic operculum within the AN, the left lingual gyrus and left para-hippocampal gyrus within the IVN, the right cuneus within pDMN, the left middle temporal gyrus within the lFPN, the right superior temporal gyrus and right insula within the two VANs (all $P<0.01$, uncorrected, cluster size > 30). Furthermore, within the dSMN, SSc patients demonstrated significantly decreased FC in the right cuneus and increased FC in the right postcentral gyrus (all $P<0.01$, uncorrected, cluster size > 30). Within the two DANs, SSc patients exhibited significantly decreased FC in the right precuneus and left middle occipital gyrus and increased FC in the right superior parietal gyrus (all $P<0.01$, uncorrected, cluster size > 30).

Functional network connectivity results

Among the 20 ICs extracted using group ICA, the FNC correlation matrix and the significant connectivity differences between ICs are illustrated in Fig. 4. Compared to healthy volunteers, SSc patients exhibited significantly decreased connectivity between several pairs of networks: the AN and the VAN (t = -2.17, $P=0.034$), the mVN and the vSMN (t = -2.02, $P=0.048$), the mVN and the VAN (t = -2.54, $P=0.014$), the lFPN and the DAN (t = -2.81, $P=0.007$), and the rFPN and the DAN (t = -3.27, $P=0.002$). Conversely, SSc patients showed significantly increased connectivity between the aDMN and the lFPN (t=2.55, $P=0.013$).

Association between clinical characteristics and fMRI measurements

The results of the associations between clinical characteristics and fMRI measurements are presented in Table 4. Notably, disease duration demonstrated significant correlations with several fMRI measurements. Specifically, negative associations were observed between disease duration and the mfALFF in the left middle frontal gyrus (r = -0.31, $P=0.041$), and between disease duration and intra-network FC of VAN in the right insula (r = -0.31, $P=0.041$), while a positive correlation was found between disease duration and ReHo in the right inferior temporal gyrus ($r=0.36$, $P=0.017$). The elevated ESR was found to be significantly associated with the FC between aDMN and lFPN ($r=0.35$, $P=0.022$).

Regarding neuropsychological assessment, the MoCA score showed a significant positive association with the FC between AN and VAN ($r=0.43$, $P=0.004$). Additionally, the HAMD score was negatively correlated with

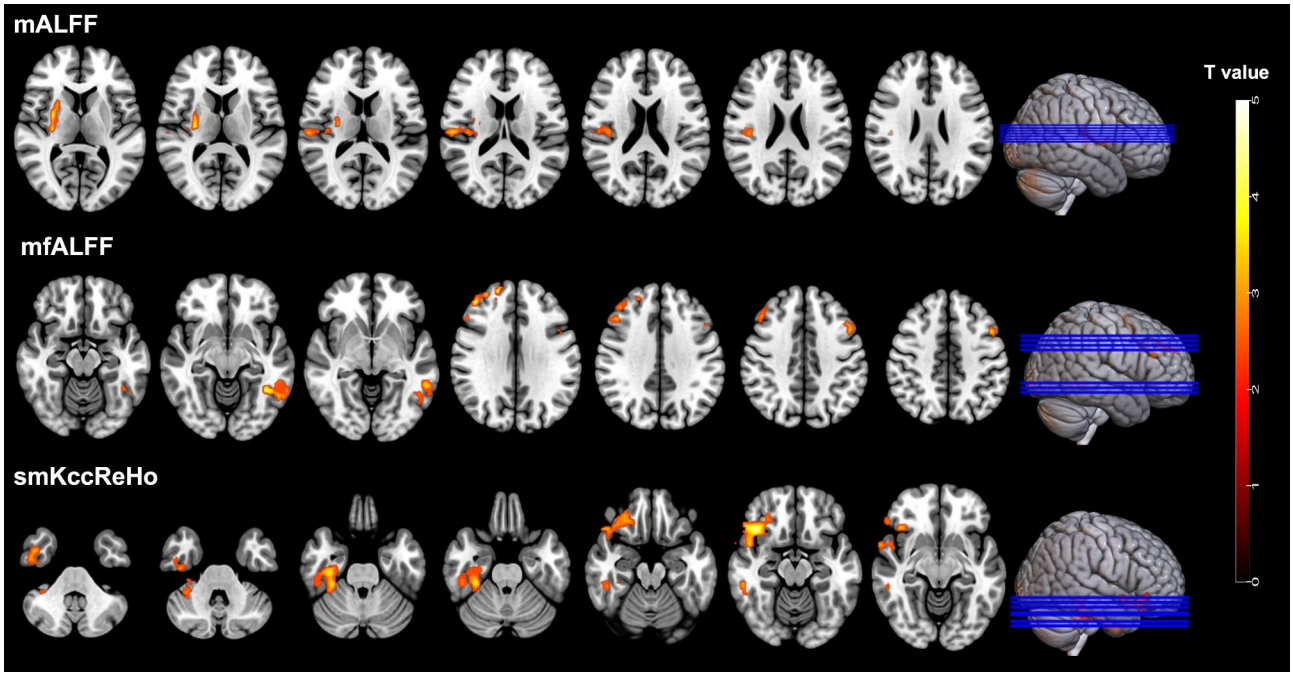

Fig. 2 Brain regions with significant differences of mALFF, mfALFF and smKccReHo between SSc patients and healthy volunteers ($P < 0.01$, FWE corrected)

Table 2 The information of brain regions with significant different ALFF and ReHo values

Cluster index	Brain regions	Cluster size	Peak t value	MNI coordinates		
				X	Y	Z
mALFF						
1	Right lenticular nucleus, putamen	139	4.36	30	-18	9
mfALFF						
1	Left inferior temporal gyrus	117	4.61	-42	-51	-9
2	Right middle frontal gyrus	105	4.31	42	42	30
3	left middle frontal gyrus	103	4.00	-48	12	42
smKccReHo						
1	Right inferior temporal gyrus	287	3.92	42	3	-45
2	Right inferior frontal gyrus, orbital part	236	4.71	42	24	-15

intra-network FC of DAN in the left middle occipital gyrus ($r = -0.40$, $P=0.007$).

In terms of clinical manifestations, Raynaud's phenomenon exhibited several associations: a negative correlation with mALFF in the putamen of the right lenticular nucleus ($r = -0.41$, $P=0.005$), a positive correlation with ReHo in the orbital part of the right inferior frontal gyrus ($r=0.31$, $P=0.043$), a negative correlation with intra-network FC of VAN in the right insula ($r = -0.31$, $P=0.043$), and a positive correlation with the FC between aDMN and lFPN ($r=0.30$, $P=0.047$). The ILD was significantly associated with both mfALFF in the left middle frontal gyrus and intra-network FC of AN in the right rolandic operculum ($r=0.36$, $P=0.017$). Additionally, The DU was significantly negatively correlated with intra-network FC of VAN in the right insula ($r = -0.42$, $P=0.004$).

Discussion

This study investigated the RS fMRI alternations in SSc patients using both functional segregation and functional integration analyses. In the functional segregation analysis, SSc patients exhibited significantly decreased mALFF and mfALFF, but increased smKccReHo, compared to healthy volunteers. In the functional integration analysis, SSc patients predominantly showed decreased intra-network and inter-network connectivity compared to healthy volunteers. The networks exhibiting above connectivity alterations included the AN, VN, DMN, FPN, DAN, and VAN. Additionally, clinical characteristics including disease duration, elevated ESR, MoCA score, HAMD score, and clinical manifestations (Raynaud's phenomenon, ILD, and DU) were significantly associated with fMRI measurements. Our findings indicate that brain function is altered in SSc patients and is associated

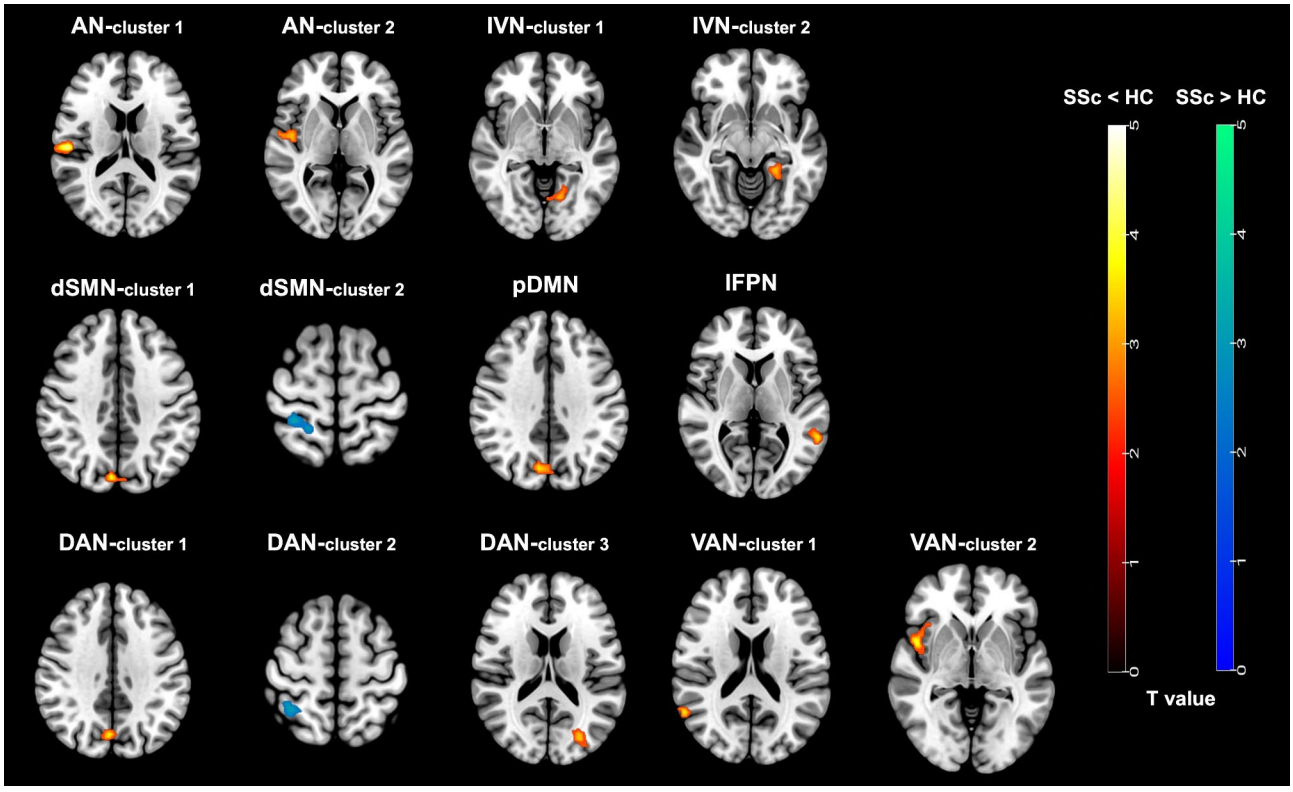

Fig. 3 Brain regions with significant differences of intra-network functional connectivity between SSc patients and healthy volunteers ($P < 0.01$, uncorrected, cluster size > 30). AN, auditory network; IVN, lateral visual network; dSMN, dorsal sensorimotor network; pDMN, posterior default mode network; IFPN, left frontoparietal network; DAN, dorsal attention network; VAN, ventral attention network

Table 3 The information of brain regions with significant different intra-network functional connectivity

Network	Contrast	Brain regions	Cluster size	Peak t value	MNI coordinates		
					X	Y	Z
AN	SSc < HC	right insula	35	3.35	45	-9	3
AN	SSc < HC	right Rolandic operculum	54	4.88	54	-21	15
IVN	SSc < HC	left lingual gyrus	34	3.53	-15	-66	-3
IVN	SSc < HC	left Para-hippocampal gyrus	41	4.04	-27	-30	-15
dSMN	SSc < HC	right cuneus	36	4.05	6	-78	36
dSMN	SSc > HC	right postcentral gyrus	42	3.38	30	-42	66
pDMN	SSc < HC	right cuneus	68	3.64	9	-75	36
IFNP	SSc < HC	left middle temporal gyrus	51	3.82	-60	-48	3
DAN-1	SSc < HC	right precuneus	30	3.88	3	-72	36
DAN-1	SSc > HC	right superior parietal gyrus	31	3.34	39	-45	57
DAN-2	SSc < HC	left middle occipital gyrus	54	3.44	-27	-78	18
VAN-1	SSc < HC	right superior temporal gyrus	33	3.91	60	-57	21
VAN-2	SSc < HC	right insula	74	4.19	48	6	-3

SSc, patients with systemic sclerosis; HC, healthy controls; AN, auditory network; IVN, lateral visual network; dSMN, dorsal sensorimotor network; pDMN, posterior default mode network; IFPN, left frontoparietal network; DAN, dorsal attention network; VAN, ventral attention network

with various clinical characteristics. This study provides new insights into the brain involvement in SSc.

In the present study, the SSc patients showed significantly decreased mALFF in the putamen and decreased mfALFF in frontal-temporal regions compared to healthy volunteers. Previous studies have shown that the putamen and frontal-temporal regions are involved in motor control, cognitive functions, and language processing [21–23]. The decreased ALFF in these areas suggests reduced spontaneous neural activity in SSc patients. In addition, we found that SSc patients showed significantly increased smKccReHo. The increase of ReHo might be due to a compensatory process to maintain normal

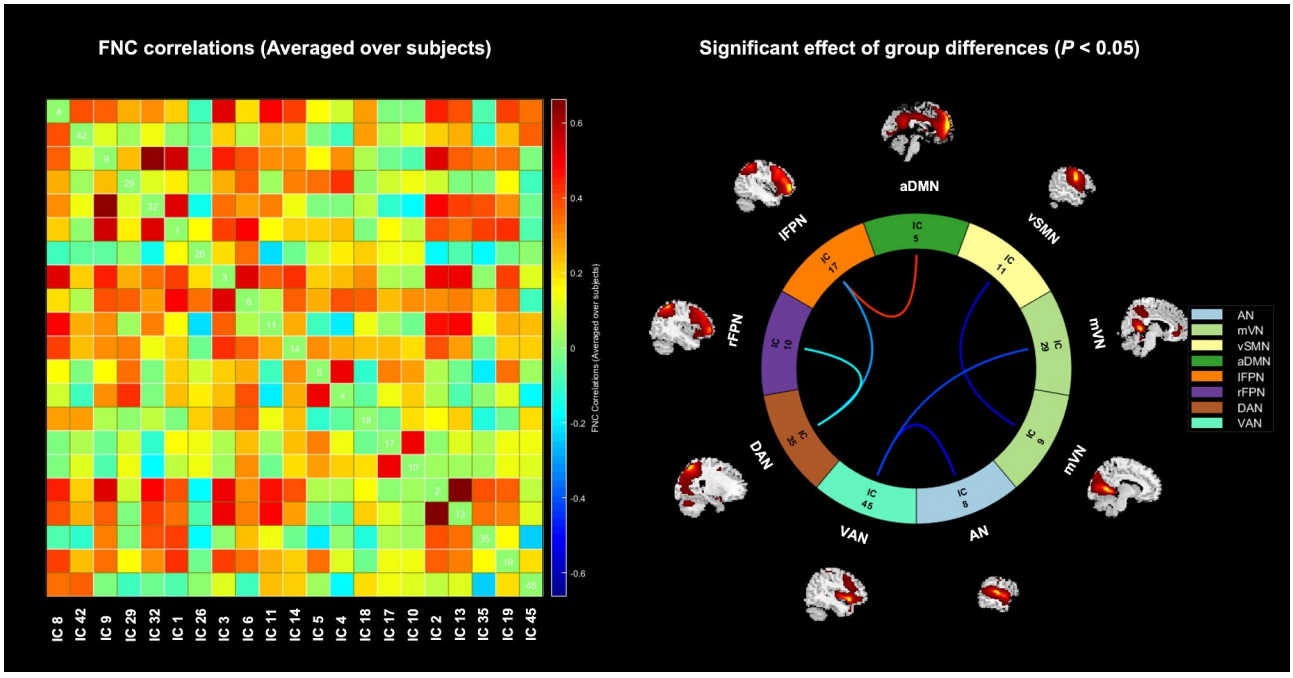

Fig. 4 The inter-network functional connectivity results. The left one represents the correlation matrix of functional network connectivity between independent components (averaged over subjects). The right one represents the functional network connection intensity differences between groups ($P < 0.05$, FDR correction). The blue line indicates lower functional connection strength in SSc patients compared to healthy volunteers, while the red line represents increase. AN, auditory network; mVN, medial visual network; vSMN, ventral sensorimotor network; aDMN, anterior default mode network; lFPN, left frontoparietal network; rFPN, right frontoparietal network; DAN, dorsal attention network; VAN, ventral attention network

Table 4 The correlation of clinical characteristics and fMRI measurements in some brain regions

fMRI measurements	Brain regions	Correlation with						
		Disease duration	MoCA	HAMD	Elevated ESR	Raynaud's phenomenon	ILD	DU
mALFF	Right lenticular nucleus, putamen	-0.19 (0.297)	0.10 (0.534)	-0.28 (0.071)	0.18 (0.254)	**-0.41 (0.005)**	0.13 (0.389)	-0.14 (0.376)
mfALFF	left middle frontal gyrus	**-0.31 (0.041)**	0.01 (0.976)	-0.02 (0.910)	0.12 (0.422)	-0.10 (0.509)	**0.35 (0.020)**	-0.23 (0.139)
ReHo	Right inferior temporal gyrus	**0.36 (0.017)**	0.15 (0.326)	-0.19 (0.211)	-0.01 (0.989)	0.27 (0.075)	-0.18 (0.248)	0.01 (0.978)
ReHo	Right inferior frontal gyrus, orbital part	0.25 (0.099)	0.20 (0.194)	0.02 (0.914)	0.02 (0.894)	**0.31 (0.043)**	-0.14 (0.358)	0.06 (0.690)
FC (AN)	right Rolandic operculum	-0.05 (0.773)	-0.04 (0.789)	-0.22 (0.161)	0.04 (0.780)	-0.02 (0.905)	**0.36 (0.017)**	0.04 (0.804)
FC (DAN)	left middle occipital gyrus	0.03 (0.849)	0.01 (0.965)	**-0.40 (0.007)**	0.18 (0.232)	0.01 (0.952)	0.26 (0.095)	0.04 (0.804)
FC (VAN)	right insula	**-0.31 (0.041)**	-0.09 (0.581)	-0.12 (0.445)	0.04 (0.780)	**-0.31 (0.043)**	0.22 (0.153)	**-0.42 (0.004)**
FC (AN-VAN)	/	0.03 (0.851)	**0.43 (0.004)**	-0.24 (0.118)	0.01 (0.989)	-0.02 (0.881)	-0.12 (0.457)	-0.26 (0.088)
FC (aDMN-lFPN)	/	0.03 (0.834)	0.15 (0.337)	-0.02 (0.905)	**0.35 (0.022)**	**0.30 (0.047)**	-0.20 (0.190)	0.12 (0.439)

MoCA, Montreal Cognitive Assessment; HAMD, Hamilton Depression Scale; FC, functional connectivity; AN, auditory network; DAN, dorsal attention network; VAN, ventral attention network; aDMN, anterior default mode network; lFPN, left frontoparietal network

function in certain brain regions through increasing the activity consistency [24].

We observed a reduction in intra-network FC across several networks, including the AN, IVN, dSMN, pDMN, lFPN, DAN and VAN, in the present study. This widespread network disruption reflects the significant impact of SSc on brain function. Specifically, the insula and Rolandic operculum in the AN are responsible for processing auditory feedback [25]. The lingual and para-hippocampal gyrus within the IVN are associated with visual memory recollection [26]. The dSMN is crucial for motor initiation and execution [27]. The decreased FC in these

regions indicates potential impairments in sensory and motor processing. Notably, our previous study identified gray matter volume reduction in the para-hippocampal region of SSc patients, underscoring its relevance in SSc-related brain involvement [5]. The DMN and FPN are involved in higher order cognition and have been broadly linked to various neurological and psychiatric disorders [28–30]. A previous study reported that the precuneus within the DMN showed decreased FC in SLE patients, and its FC was correlated with anxiety symptoms [14]. In our present study, the decreased FC was located in the cuneus, near the precuneus, suggesting similar involvement. The DAN and VAN are essential for attention-related cognition processes [31]. Reduced FC within the VAN has also been observed in SLE patients [32]. The impaired FC in DAN and VAN suggests that SSc patients may have a diminished ability to perceive external stimuli. Interestingly, we found increased intra-network FC in the dSMN and DAN. The increased FC may indicate compensatory mechanisms to preserve motor and attention function amidst the widespread network disruptions in SSc.

When investigating the FNC analysis, we found decreased FC in SSc patients primarily between the AN and the VAN, the mVN and the vSMN, the mVN and the VAN, the lFPN and the DAN, and the rFPN and the DAN. This hypoconnectivity may reflect abnormal large-scale functional interactions among these networks. The AN, mVN and vSMN are sensory processing networks, whereas the VAN, DAN, FPN (rFPN and lFPN) and the DMN are associated with higher cognitive functions [33]. The reduction in FC between the mVN and vSMN indicates impaired transmission within sensory networks, while the decreased of FC between the mVN, AN and VAN suggests that the transmission of sensory network information to the attentional network is also impaired. Furthermore, the reduction in FC between the FPN and DAN networks illustrates a disruption in the control and coordination of higher-order cognitive functions. Similarly, a reduced FC between the FPN and DAN has been observed in stroke patients with motor dysfunction, suggesting impairment in the dorsolateral prefrontal cortex's management of cognitive load required for visual attention functions [34]. Additionally, we observed increased FC between the aDMN and lFPN, which may indicate a compensatory response in higher-order cognitive networks to the lack of basic sensory information.

Furthermore, significant correlations between functional alternations (mfALFF, ReHo and FC in VAN) and disease duration can be found in the present study. This finding suggests that the brain functional involvement becomes more severe with the progression of SSc. Notably, the FC between the AN and VAN was positively correlated with MoCA score, while intra-network FC in the DAN was negatively correlated with HAMD score. The VAN is involved in the cognitive control process [35], and we hypothesize that impairment in connectivity from sensory networks to higher-order cognitive networks may contribute to the cognitive dysfunction observed in SSc patients. Additionally, the DAN is associated with emotion states [36], leading us to hypothesize that decreased DAN connectivity may contribute to the depressive symptoms observed in SSc patients. Clinical manifestations including Raynaud's phenomenon and DU are recognized as typical symptoms of microvascular dysfunction in SSc [37]. The association between these clinical manifestations and functional alternations implies that the brain may also be affected by similar impairments, which requires further investigation for validation. Furthermore, abnormal FC (increased FC between aDMN and lFPN) was positively correlated with elevated ESR. The correlation between FC and ESR has also been observed in patients with RA compelling the evidence of inflammation-induced brain damage [15]. Therefore, we hypothesize that inflammation and microvascular dysfunction in SSc contribute to the impairment of brain function, manifesting as disrupted connectivity from sensory to higher-order cognitive networks and affecting patients' cognitive and depressive states. However, it is well known that ESR levels can be influenced by various factors [38]. SSc is not primarily an inflammatory disease, and our correlation analysis did not yield significant results between brain functional characteristics and other inflammatory markers. This preliminary hypothesis warrants more neurological investigations for validation.

Several limitations in this study should be noted. Firstly, this cross-sectional study has a relatively small sample size and lacks the follow-up data to validate the proposed hypotheses. Additionally, the majority of SSc patients enrolled in our study had generally long disease duration and received medication prior to their initial visit, which may lead to symptomatic relief and relatively low mRSS (evaluated at the time of MR imaging). Secondly, this study did not compare HAMA, HAMD and MoCA scores between SSc patients and healthy volunteers because such information was not available in the healthy volunteers. Thirdly, given that our study is an initial exploratory investigation, the slightly relaxed statistical thresholds were employed. Fourthly, the present study did not consider certain potential confounding factors, such as medications taken by SSc patients (steroids and vasodilators), and their effects on brain function in this population remain unclear. Future studies are warranted to address these limitations by increasing the sample size and considering influential factors.

Conclusions

Brain functional alternations occur in SSc patients, primarily characterized by decreased spontaneous activity and functional connectivity. These alternations are partially associated with neuropsychiatric manifestations and tend to aggravate with disease duration.

Abbreviations

SSc	Systemic sclerosis
RS	Resting state
fMRI	Functional MR imaging
FC	Functional connectivity
SLE	Systemic lupus erythematosus
RA	Rheumatoid arthritis
BMI	Body mass index
lcSSc	Limited cutaneous SSc
dcSSc	Diffuse cutaneous SSc
mRSS	Modified Rodnan skin score
DU	Digital ulcers
ILD	Interstitial lung disease
ESR	Erythrocyte sedimentation rate
ANA	Antinuclear antibody
HAMA	Hamilton anxiety scale
HAMD	Hamilton depression scale
MoCA	Montreal cognitive assessment
MNI	Montreal neurological institute
ALFF	Low frequency fluctuation
FWHM	Full-width half-maximum
ReHo	Regional homogeneity
Kcc	Kendall's correlation coefficient
ICA	Independent component analysis
IC	Independent component
AN	Auditory network
mVN	Medial visual network
lVN	Lateral visual network
pVN	Posterior visual network
dSMN	Dorsal sensorimotor network
vSMN	Ventral sensorimotor network
SN	Salience network
aDMN	Anterior default mode network
pDMN	Posterior default mode network
lFPN	Left frontoparietal network
rFPN	Right frontoparietal network
DAN	Dorsal attention network
VAN	Ventral attention network
FNC	Functional network connectivity
FWE	Family-wise error
FDR	False discovery rate

Acknowledgements

We greatly thank Ms. Le He and Ms. Dan Zhao from Center for Biomedical Imaging Research, School of Biomedical Engineering, Tsinghua University, Beijing, China for their helps in MR scanning.

Author contributions

T.X. and H.H. contributed equally to this work. T.X. acquired the MR data. H.H. and X.S. acquired the clinical data. T.X. and H.H. performed the statistical analysis and drafted manuscript. S.R. and N.Z. provided technique support. W.Q., Z.X. and X.D. recruited the patients. H.Z., X.D. and Z.X. conceived and designed the experiments, conceived the overall study, handled funding and supervision, and drafted the manuscript. All authors read and approved the final manuscript.

Funding

This study was supported by the grants of National Natural Science Foundation of China (82272047, 81727807), CAMS Innovation Fund for Medical Sciences (CIFMS) (2021-I2M-1-005) and National High Level Hospital Clinical Research Funding (2022-PUMCH-B-013).

Data availability

The datasets generated and analyzed during the current study are not publicly available due to them containing information that could compromise research participant privacy/consent but are available from the corresponding author on reasonable request.

Declarations

Ethics approval and consent to participate

The Research Ethics Committee of Peking Union Medical College Hospital approved the study protocol (No. ZS-3245). All participants completed a written informed consent form.

Consent for publication

Not applicable.

Competing interests

The authors declare no competing interests.

Author details

[1]Department of Nuclear Medicine, Beijing Tsinghua Changgung Hospital, School of Clinical Medicine, Tsinghua University, Haidian District, Beijing 100084, China
[2]Department of Rheumatology,Peking Union Medical College Hospital,Peking Union Medical College and Chinese Academy of Medical Sciences,National Clinical Research Center for Dermatologic and Immunologic Diseases (NCRC-DID),Key Laboratory of Rheumatology & Clinical Immunology, Ministry of Education, Shuaifuyuan, Dongcheng District, Beijing 100730, China
[3]Center for Biomedical Imaging Research, School of Biomedical Engineering, Tsinghua University, Haidian District, Beijing 100084, China
[4]Department of Perinatal Imaging and Health, King's College London, London SE1 7EH, UK

Received: 9 September 2024 / Accepted: 4 November 2024
Published online: 08 November 2024

References

1. Volkmann ER, Andréasson K, Smith V. Systemic sclerosis. Lancet. 2023;401:304–18.
2. Perelas A, Silver RM, Arrossi AV, et al. Systemic sclerosis-associated interstitial lung disease. Lancet Respir Med. 2020;8:304–20.
3. He H, Tong X, Ning Z, et al. Diffusing capacity of lungs for carbon monoxide associated with subclinical myocardial impairment in systemic sclerosis: a cardiac MR study. RMD Open. 2023;9:e003391.
4. Tong X, He H, Ning Z, et al. Characterization of kidneys in patients with systemic sclerosis by multi-parametric magnetic resonance quantitative imaging. Magn Reson Imaging. 2024;109:203–10.
5. Tong X, He H, Xu S et al. Changes of cerebral structure and perfusion in subtypes of systemic sclerosis: a brain magnetic resonance imaging study. Rheumatology (Oxford) 2024;keae404.
6. Sakr BR, Rabea RE, Aboulfotooh AM, et al. Neurosonological and cognitive screening for evaluation of systemic sclerosis patients. Clin Rheumatol. 2019;38:1905–16.
7. Gamal RM, Abozaid HSM, Zidan M, et al. Study of MRI brain findings and carotid US features in systemic sclerosis patients, relationship with disease parameters. Arthritis Res Ther. 2019;21(1):95.
8. Chen YT, Lescoat A, Khanna D, et al. Perceived cognitive function in people with systemic sclerosis: associations with symptoms and Daily Life Functioning. Arthritis Care Res. 2023;75:1706–14.
9. Chen YT, Lescoat A, Devine A, et al. Cognitive difficulties in people with systemic sclerosis: a qualitative study. Rheumatology (Oxford). 2022;61:3754–65.
10. Oláh C, Schwartz N, Denton C, et al. Cognitive dysfunction in autoimmune rheumatic diseases. Arthritis Res Ther. 2020;22:78.
11. Wuriliga, Xu D, He Y, et al. Mild cognitive impairment in patients with systemic sclerosis and features analysis. Rheumatology. 2022;61:2457–63.
12. Tononi G, Sporns O, Edelman GM. A measure for brain complexity: relating functional segregation and integration in the nervous system. Proc Natl Acad Sci U S A. 1994;91:5033–7.

13. Yang Y, Zhao R, Zhang F, et al. Dynamic changes of amplitude of low-frequency in systemic lupus erythematosus patients with cognitive impairment. Front Neurosci. 2022;16:929383.
14. Bonacchi R, Rocca MA, Ramirez GA, et al. Resting state network functional connectivity abnormalities in systemic lupus erythematosus: correlations with neuropsychiatric impairment. Mol Psychiatry. 2021;26:3634–45.
15. Zheng Y, Hou Z, Ma S, et al. Altered dynamic functional network connectivity in rheumatoid arthritis associated with peripheral inflammation and neuropsychiatric disorders. RMD Open. 2024;10:e003684.
16. van den Hoogen F, Khanna D, Fransen J, et al. 2013 classification criteria for systemic sclerosis: an American college of rheumatology/European league against rheumatism collaborative initiative. Ann Rheum Dis. 2013;72:1747–55.
17. Hamilton M. The assessment of anxiety states by rating. Br J Med Psychol. 1959;32:50–5.
18. Hamilton M. A rating scale for depression. J Neurol Neurosurg Psychiatry. 1960;23:56–62.
19. Nasreddine ZS, Phillips NA, Bédirian V, et al. The Montreal Cognitive Assessment, MoCA: a brief screening tool for mild cognitive impairment. J Am Geriatr Soc. 2005;53:695–9.
20. Cai H, Wang C, Qian Y, et al. Large-scale functional network connectivity mediate the associations of gut microbiota with sleep quality and executive functions. Hum Brain Mapp. 2021;42:3088–101.
21. Arsalidou M, Duerden EG, Taylor MJ. The centre of the brain: topographical model of motor, cognitive, affective, and somatosensory functions of the basal ganglia. Hum Brain Mapp. 2013;34:3031–54.
22. Zhang L, Li B, Wang H, et al. Decreased middle temporal gyrus connectivity in the language network in schizophrenia patients with auditory verbal hallucinations. Neurosci Lett. 2017;653:177–82.
23. Hofmann W, Schmeichel BJ, Baddeley AD. Executive functions and self-regulation. Trends Cogn Sci. 2012;16:174–80.
24. Pan P, Zhan H, Xia M, et al. Aberrant regional homogeneity in Parkinson's disease: a voxel-wise meta-analysis of resting-state functional magnetic resonance imaging studies. Neurosci Biobehav Rev. 2017;72:223–31.
25. Golden HL, Agustus JL, Nicholas JM, et al. Functional neuroanatomy of spatial sound processing in Alzheimer's disease. Neurobiol Aging. 2016;39:154–64.
26. Fateh AA, Long Z, Duan X, et al. Hippocampal functional connectivity-based discrimination between bipolar and major depressive disorders. Psychiatry Res Neuroimaging. 2019;284:53–60.
27. Raichle ME. The restless brain. Brain Connect. 2011;1:3–12.
28. Preziosa P, Rocca MA, Ramirez GA, et al. Structural and functional brain connectomes in patients with systemic lupus erythematosus. Eur J Neurol. 2020;27:113–e2.
29. Valsasina P, Hidalgo de la Cruz M, Filippi M, et al. Characterizing Rapid fluctuations of resting state functional connectivity in demyelinating, neurodegenerative, and Psychiatric conditions: from static to time-varying analysis. Front Neurosci. 2019;13:618.
30. Baker JT, Dillon DG, Patrick LM, et al. Functional connectomics of affective and psychotic pathology. Proc Natl Acad Sci U S A. 2019;116:9050–9.
31. Corbetta M, Shulman GL. Control of goal-directed and stimulus-driven attention in the brain. Nat Rev Neurosci. 2002;3:201–15.
32. Cao ZY, Wang N, Wei H, et al. The altered functional modular organization in systemic lupus erythematosus: an independent component analysis study. Brain Imaging Behav. 2022;16:728–37.
33. Luan Y, Wang C, Jiao Y, et al. Dysconnectivity of multiple resting-state networks Associated with higher-order functions in Sensorineural hearing loss. Front Neurosci. 2019;13:55.
34. Zhao Z, Wu J, Fan M, et al. Altered intra- and inter-network functional coupling of resting-state networks associated with motor dysfunction in stroke. Hum Brain Mapp. 2018;39:3388–97.
35. Proskovec AL, Wiesman AI, Wilson TW. The strength of alpha and Gamma oscillations predicts behavioral switch costs. NeuroImage. 2019;188:274–81.
36. Salehi M, Karbasi A, Barron DS, et al. Individualized functional networks reconfigure with cognitive state. NeuroImage. 2020;206:116233.
37. Denton CP, Khanna D. Systemic sclerosis. Lancet. 2017;390:1685–99.
38. Erikssen G, Liestøl K, Bjørnholt JV, et al. Erythrocyte sedimentation rate: a possible marker of atherosclerosis and a strong predictor of coronary heart disease mortality. Eur Heart J. 2000;21(19):1614–20.

Publisher's note

Springer Nature remains neutral with regard to jurisdictional claims in published maps and institutional affiliations.